2021 43rd Annual International Conference of the
IEEE Engineering in Medicine & Biology Society (EMBC)
Oct 31 - Nov 4, 2021. Virtual Conference

Unravelling Causal Relationships Between Cortex and Muscle with Errors-in-variables Models

Zhenghao Guo[1], Verity M. McClelland[2], and Zoran Cvetkovic[1]

Abstract— **Corticomuscular communications are commonly estimated by Granger causality (GC) or directed coherence, with the aim of assessing the linear causal relationship between electroencephalogram (EEG) and electromyogram (EMG) signals. However, conventional GC based on standard linear regression (LR) models may be substantially underestimated in the presence of noise in both EEG and EMG signals: some healthy subjects with good motor skills show no significant GC. In this study, errors-in-variables (EIV) models are investigated for the purpose of estimating underlying linear time-invariant systems in the context of GC. The performance of the proposed method is evaluated using both simulated data and neurophysiological recordings, and compared with conventional GC. It is demonstrated that the inferred EIV-based causality offers an advantage over typical LR-based GC when detecting communication between the cortex and periphery using noisy EMG and EEG signals.**

I. INTRODUCTION

Dynamic interactions between cortex and muscle are commonly detected and quantified by analysing electroencephalogram (EEG) and electromyogram (EMG) signals recorded synchronously during motor tasks. The traditional measure for quantifying linear interdependencies between EEG and EMG is mainly based on the spectral methodology of corticomuscular coherence (CMC) analysis [1], [2]. To further identify the causal relationships, Granger causality (GC, or directed coherence) [3], [4] is also applied [5].

However, both CMC and GC are often not sufficiently sensitive: for some healthy subjects with good motor skills, the values of coherence and GC may even fall below the significance threshold [5]. This can be attributed to the presence of high levels of noise and activities irrelevant to studied processes in EEG and EMG signals, which are not explicitly accounted for in CMC and GC analysis [6]. The standard method of computing GC involves estimation of parameters of conventional linear regression (LR) models, including autoregressive moving average (ARMA) and autoregressive (AR) models [7]. The corresponding regression coefficients are estimated by ordinary least squares (OLS) model fitting [8]. In this case, LR models assume that the regressors have been measured exactly [9]. However, given that both EEG and EMG are noisy signals, the additive input noise may substantially modify the structure of the series, leading to underestimated or spurious causality [10]. Therefore, it is essential to account for measurement errors in both the independent and dependent variables [11], so as to have a better understanding of the causal relationship between the noise-free cortical events and noise-free muscle events.

Representations where measurement noises are presented on both independent and dependent variables are known as errors-in-variables (EIV) models [12]. Although the EIV approach is most pertinent to describing neurophysiological recordings, the interaction between EEG and EMG is seldom studied in this framework. Towards exploring the causal relationship between noisy EEG and EMG data, we propose a new concept of causality measurement, which combines traditional GC with estimation of underlying systems in the EIV framework. In the EIV framework, the model coefficients can be estimated via total least squares (TLS) approximation. In contrast to GC with OLS estimator, our EIV-based causality measurement with TLS estimation models the noise components in both input and output signals explicitly [9], [13], and hence has the potential to be advantageous for discriminating GC in the context of cortex-muscle interactions (CMI). The performance of the inferred method is evaluated using both simulated data and neurophysiological recordings, and is compared to the traditional GC measurement.

The remainder of this paper is organized as follows: Section II describes the models and the proposed methods. Section III presents the experimental results using both simulated and neurophysiological data. Section IV draws conclusions.

II. METHODS

A. The Model of CMI System

1) Standard LR model: In the basic LR model, the cortical signal $x(t)$ effects a muscle response in a linear time-invariant fashion, which is observed to be degraded by additive noise $\varepsilon_y(t)$. This is described as a moving average (MA) model $y(t) = \sum_{i=1}^{m} a_{yx,i}x(t-i) + \varepsilon_y(t)$, where $y(t)$ is the observed muscle signal. Considering the lagged interactions between EEG and EMG signals [6], the MA model can be modified to account for an arbitrary interaction delay $u \geq 0$ as $y(t+u) = \sum_{i=1}^{m} a_{yx,i}x(t-i) + \varepsilon_y(t+u)$. In a more general case of bidirectional communication, the underlying ARMA model has the form

$$x(t+u) = \sum_{i=1}^{m} a_{xx,i}x(t-i+u) + \sum_{i=1}^{m} a_{xy,i}y(t-i) + \varepsilon_x(t+u), \tag{1a}$$

$$y(t+u) = \sum_{i=1}^{m} a_{yy,i}y(t-i+u) + \sum_{i=1}^{m} a_{yx,i}x(t-i) + \varepsilon_y(t+u). \tag{1b}$$

[1]Zhenghao Guo and Zoran Cvetkovic are with Department of Engineering, King's College London, The strand, London, WC2B 4BG, UK. zhenghao.guo@kcl.ac.uk, zoran.cvetkovic@kcl.ac.uk

[2]Verity M. McClelland is with Department of Basic and Clinical Neuroscience, King's College London. verity.mcclelland@kcl.ac.uk

Models (1a) and (1b) are usually solved via OLS model fitting. To elaborate, considering the model (1b) only, parameters $a_{yy,i}$ and $a_{yx,i}$ are estimated using maximum likelihood estimation (MLE) assuming Gaussian residuals. That gives rise to the least squares model fitting. Accordingly, the coefficients $a_{yy,i}$ and $a_{yx,i}$ of the model (1b) are chosen so as to minimize the square error $E_y = (1/(N-m-u))\sum_{t=m+1}^{N-u}|\varepsilon_y(t+u)|^2$, where the number of observations of each process is N, and $\varepsilon_y(t+u) = y(t+u) - \sum_{i=1}^{m} a_{yx,i}x(t-i) - \sum_{i=1}^{m} a_{yy,i}y(t-i+u)$. An appropriate model order m is determined using the model selection criteria - Bayesian Information Criterion (BIC) [14].

2) EIV model: Compared to conventional LR models, EIV methods perform estimation of CMI systems by explicitly modelling the noise components in both input and output signals. A typical EIV model of a CMI system is given as

$$\begin{aligned} x(t+u) =& \sum_{i=1}^{m} a_{xx,i}\left(x(t-i+u) - \varepsilon_x(t-i+u)\right) + \\ &+ \sum_{i=1}^{m} a_{xy,i}\left(y(t-i) - \varepsilon_y(t-i)\right) + \varepsilon_x(t+u), \end{aligned} \tag{2a}$$

$$\begin{aligned} y(t+u) =& \sum_{i=1}^{m} a_{yy,i}\left(y(t-i+u) - \varepsilon_y(t-i+u)\right) + \\ &+ \sum_{i=1}^{m} a_{yx,i}\left(x(t-i) - \varepsilon_x(t-i)\right) + \varepsilon_y(t+u), \end{aligned} \tag{2b}$$

which gives rise to TLS model fitting. The classical solution of TLS is using singular value decomposition (SVD) [15]. Considering the model (2b) only, to simplify the notation, we first let

$$\begin{aligned} A =& [a_{yy,1}, ..., a_{yy,m}, a_{yx,1}, ..., a_{yx,m}]^{\mathrm{T}} \in \mathbb{R}^{2m\times 1}, \\ Z =& [\boldsymbol{y}(m+u), ..., \boldsymbol{y}(1+u), \\ & \boldsymbol{x}(m), ..., \boldsymbol{x}(1)] \in \mathbb{R}^{(N-m-u)\times 2m}, \\ \Delta Z =& [-\boldsymbol{\varepsilon_y}(m+u), ..., -\boldsymbol{\varepsilon_y}(1+u), \\ & -\boldsymbol{\varepsilon_x}(m), ..., -\boldsymbol{\varepsilon_x}(1)] \in \mathbb{R}^{(N-m-u)\times 2m}, \\ Y =& [\boldsymbol{y}(m+u+1)] \in \mathbb{R}^{(N-m-u)\times 1}, \\ \Delta Y =& [\boldsymbol{\varepsilon_y}(m+u+1)] \in \mathbb{R}^{(N-m-u)\times 1}, \end{aligned}$$

where we use the notation

$$\boldsymbol{y}(t) = [y(t), y(t+1), ..., y(t+N-m-u-1)]^{\mathrm{T}},$$

and analogously for $\boldsymbol{x}(t)$, $\boldsymbol{\varepsilon_y}(t)$, and $\boldsymbol{\varepsilon_x}(t)$. The EIV model (2b) can be rewritten in the matrix form as

$$Y = (Z + \Delta Z)A + \Delta Y. \tag{3}$$

Let the augmented data matrix $D = [Z, Y] = U\Sigma V^T$, where $\Sigma = \mathrm{diag}(\sigma_1, ..., \sigma_{2m+1})$ is a singular value decomposition of D, $\sigma_1 \geq \cdots \sigma_{2m+1}$ are the singular values of D, and define the partitioning

$$V = \begin{bmatrix} V_{11} & V_{12} \\ V_{21} & V_{22} \end{bmatrix} \in \mathbb{R}^{(2m+1)\times(2m+1)},$$

where V_{22} is a (1×1) matrix. If $V_{22} \neq 0$ and $\sigma_{2m} \neq \sigma_{2m+1}$, the unique TLS solution is given as $\hat{A}_{\mathrm{tls}} = -V_{12}V_{22}^{-1}$, and the corresponding TLS correction data matrix is $\Delta D_{\mathrm{tls}} = [\Delta Z, \Delta Y] = -U\,\mathrm{diag}\,(0, \sigma_{2m+1})\,V^{\mathrm{T}}$.

B. Classic GC Analysis

GC is a standard technique for measuring the causal dependence between two time series [8]. Considering the model (1b) alone, the variance of $\{\varepsilon_y(t+u)\}$, denoted as $\mathrm{Var}[\{\varepsilon_y(t+u)\}]$, determines the regression error for $y(t+u)$ based on the past samples $(y(t-m+u), ..., y(t-1+u))$ and $(x(t-m), ..., x(t-1))$. GC compares this prediction error with that obtained by predicting $y(t+u)$ based only on the past samples $(y(t-m+u), ..., y(t-1+u))$ according to the AR model

$$y(t+u) = \sum_{i=1}^{m} a'_{yy,i}y(t-i+u) + \varepsilon'_y(t+u), \tag{4}$$

where $\{\varepsilon'_y(t+u)\}$ is assumed to be zero-mean with variance $\mathrm{Var}[\{\varepsilon'_y(t+u)\}]$. If the prediction error $\mathrm{Var}[\{\varepsilon'_y(t+u)\}]$ for the AR model (4) is larger than the error $\mathrm{Var}[\{\varepsilon_y(t+u)\}]$ for the ARMA model (1b), then $\{x(t)\}$ is considered to cause $\{y(t)\}$ in terms of GC. Time-domain Granger causal influence is thus measured by the ratio

$$\mathrm{GC}_{\mathrm{ols},x\to y} = \ln \frac{\mathrm{Var}\left[\{\varepsilon'_y(t+u)\}\right]}{\mathrm{Var}\left[\{\varepsilon_y(t+u)\}\right]}, \tag{5}$$

where the residual variance $\mathrm{Var}[\{\varepsilon_y(t+u)\}]$ for ARMA model (1b) is usually estimated as the sample variance as $\mathrm{Var}[\{\varepsilon_y(t+u)\}] = \frac{1}{N-m-u-1}\sum_{t=m+1}^{N-u}|\varepsilon_y(t+u)|^2$. Similar for $\mathrm{Var}\left[\{\varepsilon'_y(t+u)\}\right]$ for AR model (4).

C. EIV-based Causality Measurement

To account for the causal relationship between two noisy signals, we then revise the traditional GC concept on the basis of the EIV model. Consider the standard linear regression model $Y = ZA + \Delta Y$, where Y, Z, A, and ΔY are defined as in model (3). The OLS approximation $\hat{A}_{\mathrm{ols}}$ for A is obtained by

$$\begin{aligned} &\left\{\hat{A}_{\mathrm{ols}}, \Delta Y_{\mathrm{ols}}\right\} = \arg\min_{A,\Delta Y} \|\Delta Y\|_2, \\ &\text{subject} \quad \text{to} \quad Y = ZA + \Delta Y, \end{aligned} \tag{6}$$

which aims to correct the residual ΔY as little as possible in terms of the Euclidean norm. Standard GC thus quantifies the increase of prediction error (the sample variance or unbiased mean square of the Euclidean norm of the residual ΔY), when the vectors $\boldsymbol{x}(m), ..., \boldsymbol{x}(1)$ are excluded from Z in the corresponding AR model $Y = Z'A' + \Delta Y'$. Here,

$$\begin{aligned} A' =& \left[a'_{yy,1}, a'_{yy,2}, ..., a'_{yy,m}\right]^{\mathrm{T}} \in \mathbb{R}^{m\times 1}, \\ Z' =& [\boldsymbol{y}(m+u), ..., \boldsymbol{y}(1+u)] \in \mathbb{R}^{(N-m-u)\times m}, \\ \Delta Y' =& [\boldsymbol{\varepsilon'_y}(m+u+1)] \in \mathbb{R}^{(N-m-u)\times 1}, \end{aligned}$$

where

$$\boldsymbol{\varepsilon'_y}(t) = [\varepsilon'_y(t), \varepsilon'_y(t+1), ..., \varepsilon'_y(t+N-m-u-1)]^{\mathrm{T}}.$$

In the context of the EIV model, considering the equation (3), the TLS approximation $\hat{A}_{\text{tls}}$ for A is given by

$$\left\{\hat{A}_{\text{tls}}, \Delta Z_{\text{tls}}, \Delta Y_{\text{tls}}\right\} = \arg \min_{A,\Delta Z,\Delta Y} \|[\Delta Z, \Delta Y]\|_{\text{F}}, \quad \text{subject to} \quad Y = (Z + \Delta Z)A + \Delta Y, \tag{7}$$

which looks for the minimal corrections for both ΔZ and ΔY in the Frobenius norm sense. This motivates the use of the unbiased mean square of the Frobenius norm of $[\Delta Z, \Delta Y]$ to quantify the increase in error in both the independent and dependent variables, when the vectors $\boldsymbol{x}(m), ..., \boldsymbol{x}(1)$ and $-\boldsymbol{\varepsilon_x}(m), ..., -\boldsymbol{\varepsilon_x}(1)$ are excluded from Z and ΔZ, respectively, in the corresponding AR model $Y = (Z' + \Delta Z')A' + \Delta Y'$. Here,

$$\Delta Z' = [-\boldsymbol{\varepsilon_y}(m+u), ..., -\boldsymbol{\varepsilon_y}(1+u)] \in \mathbb{R}^{(N-m-u)\times m},$$

The EIV-based causality can thus be defined as

$$\text{C}_{\text{tls},x\to y} = \ln \frac{\frac{1}{(N-m-u)(m+1)-1}\|[\Delta Z', \Delta Y']\|_{\text{F}}^2}{\frac{1}{(N-m-u)(2m+1)-1}\|[\Delta Z, \Delta Y]\|_{\text{F}}^2}. \tag{8}$$

D. Statistical testing

We used independent Gaussian sequences to identify significant values of causality. A total of 1000 pairs of Gaussian independent signals were produced with the variances equal to the variances of investigated simulated and neurophysiological signals. Then the above two methods were followed. For the approximately normal distributed result values, we use two standard deviations of the mean as the thresholds, which approximates to a 95% confidence level (CL). Values larger than these identified thresholds will be regarded as significant.

III. RESULTS

A. Simulated Data Results

Let us consider a linear system between two time series $\{x_0(t)\}$ and $\{y_0(t)\}$, where $\{y_0(t)\}$ depends on $\{x_0(t)\}$, and $\{x_0(t)\}$ is independent of $\{y_0(t)\}$:

$$x_0(t) = 0.95\sqrt{2}x_0(t-1) - 0.9025x_0(t-2), \tag{9a}$$

$$y_0(t) = -0.5y_0(t-3) + 2x_0(t-1) + 1.6x_0(t-2). \tag{9b}$$

Let us further consider estimating this system and the underlying causality relationships from noisy observations $x(t) = x_0(t) + \varepsilon_x(t)$ and $y(t) = y_0(t) + \varepsilon_y(t)$, where $\{\varepsilon_x(t)\}$ and $\{\varepsilon_y(t)\}$ are Gaussian noise sequences with a mean of 0 and a standard deviation of 0.1. We evaluate the proposed methodology using a $N = 50$ samples' long realization of $\{x(t)\}$ and $\{y(t)\}$.

The coefficient estimation results of model (9b) are shown in Table I, where the relative error of estimation is computed as $\|\hat{\boldsymbol{a}} - \boldsymbol{a}\|_2/\|\boldsymbol{a}\|_2$, for $\boldsymbol{a} = [a_1, ..., a_{n_p}]^{\text{T}}$, and n_p is the number of parameters. According to the table, the TLS method gives better parametric estimation. This is due to the presence of noise in both $\{x(t)\}$ and $\{y(t)\}$ such that the OLS method, in which the independent variables are assumed to be error-free, gives a worse estimation.

TABLE I

THE COEFFICIENT ESTIMATION OF MODEL (9B), $\text{SNR}_{\boldsymbol{x}} = 7.39\text{dB}$.

	a_1	a_2	a_3	a_4	a_5	a_6	relative error
$\boldsymbol{a}$	2	1.6	0	0	0	-0.5	0
$\hat{\boldsymbol{a}}_{\text{ols}}$	1.41	1.25	0.03	0.17	0	-0.53	0.27
$\hat{\boldsymbol{a}}_{\text{tls}}$	2.08	1.56	0.09	0.01	0.02	-0.48	0.05

The causality results are shown in Table II. The classic GC detects a significant directed connection from $\{x(t)\}$ to $\{y(t)\}$ ($1.15 > 0.19$); whist GC from $\{y(t)\}$ to $\{x(t)\}$ is close to the significant level ($0.20 \approx 0.19$). In contrast, our EIV-based method successfully detects significant causality from $\{x(t)\}$ to $\{y(t)\}$ ($2.89 > 1.36$ and $0.63 < 1.36$), which confirms the inferred EIV-based causality method for measuring causality in the EIV context.

TABLE II

CAUSALITY BETWEEN $\{x(t)\}$ AND $\{y(t)\}$.

	GC		EIV-based causality	
	x **to** y	y **to** x	x **to** y	y **to** x
Causality	1.15	0.20	2.89	0.63
Significant level	0.19	0.19	1.36	1.36

B. Results on Neurophysiological Data

1) Data Collection: The above method was applied to neurophysiological recordings collected from four healthy subjects during a controlled movement task [2]. The subjects gave informed consent to the study, which was ethically approved and carried out in accordance with the declaration of Helsinki. The subjects were asked to sit at a table, and hold a 15 cm ruler with the thumb and index finger of the right hand, grasping the end 2 cm of the ruler, and keeping the ruler 2 cm above and parallel to the tabletop. The disturbance was provided by an electromechanical tapper. The length of each trial was 5 s, and the stimulus was given 1.1 s after the start of the trial. The entire experiment consisted of up to 8 blocks of 25 trials each. Thus, approximately 200 trials of data were collected from each subject. EEG was recorded from the scalp overlying the contralateral hand area of the motor cortex. EMG was recorded over the first dorsal interosseous (FDI) muscle of the dominant hand. The sampling frequency was 1024 Hz. Raw data were reviewed offline by visual inspection, and epochs of data with blink artefacts or movement were rejected [2].

2) GC results: In this study, all GC analysis was performed within 500 ms (512 samples) segments every 250 ms (256 samples). The model order m is determined by BIC [14] which gave $m = 30$. In addition to the model order, in neuroscience, interaction delays u can amount to several tens of milliseconds. For the EEG-EMG coupling analysis, the interaction delay is estimated to be between 20 and 35 milliseconds (ms) [6]. In this study, u is set to correspond to the number of samples in 25 ms for both directions.

The result of GC analysis is shown in Figure 1. According to Figure 1, Subjects A and B present significant bidirectional GC almost throughout the experiments, especially in the

direction of EEG→EMG. In contrast, for subjects C and D, the value of GC fluctuates around the 95% CL, which exhibits an inconsistent result across subjects.

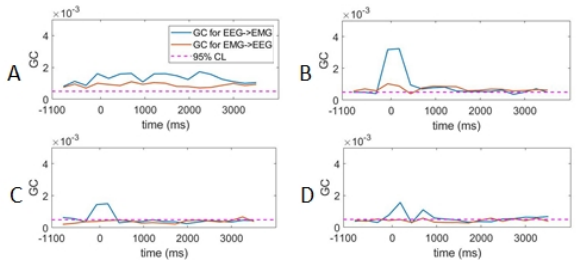

Fig. 1. GC in subjects A-D, showing changes in GC over time. The stimulus is set at $t = 0$.

3) EIV-based causality results: Similar to GC analysis, the inferred EIV-based causality analysis was performed using the same parameters. Figure 2(a) shows the EIV-based causality results: TLS-causality reveals communication in the direction from EEG to EMG with a consistent pattern across subjects A-D; while it is not significant in the opposite direction. The observations suggest that, in the context of an EIV model, linear causality is more prominent for communication from EEG to EMG. In a study of cross-frequency coupling using a modified CMC method, Yang *et al.* also found evidence for predominantly linear coupling in the cortex-muscle direction, whereas there are more non-linear dynamics in sensory feedback pathways [16]. Our findings with TLS-causality are thus concordant with this.

To further show changes in EIV-based causality over time, Figure 2(b) presents the zoomed-in EIV-based causality in the direction of EEG→EMG. A fluctuation in the level of causality in relation to the stimulus is observed, and all the subjects show high causality during the post-stimulus period.

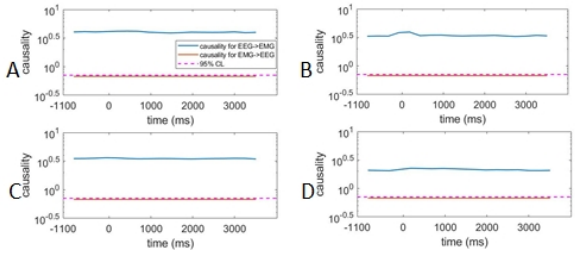

(a) EIV-based causality. The y-axis is set as log-scale.

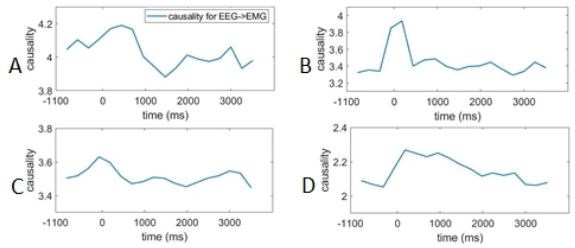

(b) Zoomed-in EIV-based causality from EEG to EMG.

Fig. 2. EIV-based causality in subjects A-D, showing changes in EIV-based causality over time. The stimulus is set at $t = 0$.

IV. CONCLUSIONS

In this study, EIV models are introduced to account for measurement noise in both the input and output signals of a CMI system. We propose a novel causality measurement based on the EIV models, along with the TLS solution. Using simulated data, we demonstrate that the EIV-based causality method would successfully detect the causal relationship between two time series in an EIV problem. Evaluations using neurophysiological data indicate that the method is potentially advantageous for detecting GC relationships in the context of CMI.

REFERENCES

[1] SN Baker, Etienne Olivier, and RN Lemon. Coherent oscillations in monkey motor cortex and hand muscle EMG show task-dependent modulation. *The Journal of physiology*, 501(1):225–241, 1997.

[2] Verity M McClelland, Zoran Cvetkovic, and Kerry R Mills. Modulation of corticomuscular coherence by peripheral stimuli. *Experimental brain research*, 219(2):275–292, 2012.

[3] Clive WJ Granger. Investigating causal relations by econometric models and cross-spectral methods. *Econometrica: journal of the Econometric Society*, pages 424–438, 1969.

[4] Luiz A Baccalá and Koichi Sameshima. Partial directed coherence: a new concept in neural structure determination. *Biological cybernetics*, 84(6):463–474, 2001.

[5] Claire L Witham, C Nicholas Riddle, Mark R Baker, and Stuart N Baker. Contributions of descending and ascending pathways to corticomuscular coherence in humans. *The Journal of physiology*, 589(15):3789–3800, 2011.

[6] Yuhang Xu, Verity M McClelland, Zoran Cvetković, and Kerry R Mills. Corticomuscular coherence with time lag with application to delay estimation. *IEEE Transactions on Biomedical Engineering*, 64(3):588–600, 2016.

[7] John Geweke. Measurement of linear dependence and feedback between multiple time series. *Journal of the American statistical association*, 77(378):304–313, 1982.

[8] Lionel Barnett and Anil K Seth. The MVGC multivariate Granger causality toolbox: a new approach to Granger-causal inference. *Journal of neuroscience methods*, 223:50–68, 2014.

[9] Ivan Markovsky and Sabine Van Huffel. Overview of total least-squares methods. *Signal processing*, 87(10):2283–2302, 2007.

[10] Brian DO Anderson, Manfred Deistler, and Jean-Marie Dufour. On the sensitivity of Granger causality to errors-in-variables, linear transformations and subsampling. *Journal of Time Series Analysis*, 40(1):102–123, 2019.

[11] Clark Glymour, Kun Zhang, and Peter Spirtes. Review of causal discovery methods based on graphical models. *Frontiers in genetics*, 10:524, 2019.

[12] Torsten Söderström. Errors-in-variables methods in system identification. *Automatica*, 43(6):939–958, 2007.

[13] Sabine Van Huffel and Philippe Lemmerling. *Total least squares and errors-in-variables modeling: analysis, algorithms and applications*. Springer Science & Business Media, 2013.

[14] Gideon Schwarz et al. Estimating the dimension of a model. *The annals of statistics*, 6(2):461–464, 1978.

[15] Gene H Golub and Charles F Van Loan. An analysis of the total least squares problem. *SIAM journal on numerical analysis*, 17(6):883–893, 1980.

[16] Yuan Yang, Teodoro Solis-Escalante, Mark van de Ruit, Frans CT van der Helm, and Alfred C Schouten. Nonlinear coupling between cortical oscillations and muscle activity during isotonic wrist flexion. *Frontiers in computational neuroscience*, 10:126, 2016.